

Downregulation of MicroRNA-29-3p Following Percutaneous Coronary Intervention: An Implication of YY1/IRAK1 Pathway in the Post-Vascular Injury Inflammation

Yunying Zhou,^{1#} Yong Yang,^{2#} Lang Hong,¹ Liang Shao,¹ Hengli Lai,¹ Fangxin Zhu¹ and Jianyun Lan¹

This study explored the expression of microRNA (miR)-29b-3p following percutaneous coronary intervention (PCI) and the implication of its downstream Yin Yang 1 (YY1)/interleukin (IL)-1 receptor-associated kinase 1 (IRAK1) pathway in post-vascular injury inflammation. Blood samples were collected for analysis of plasma miR-29b-3p from patients with acute coronary syndrome before surgery, 1 day after PCI, and 30 days after PCI. Lipopolysaccharide (LPS)-treated human coronary artery endothelial cells (HCAECs) were transfected with miR-29b-3p mimic/inhibitor or YY1 shRNA and underwent viability tests. Enzyme-linked immunosorbent assay was performed to detect the levels of soluble vascular cell adhesion molecule-1 (sVCAM-1), IL-1 β , IL-6, and tumor necrosis factor (TNF)- α in serum and cell culture supernatant. Dual-luciferase reporter and RNA/chromatin immunoprecipitation were used to confirm the targeting relationships among miR-29b-3p, YY1, and IRAK1. A rat model of intraluminal injury of the common femoral artery was established to address the role of miR-29b-3p and relevant mechanisms. miR-29b-3p was lowly expressed, and sVCAM-1, IL-1 β , IL-6, and TNF- α were upregulated 1 day after PCI and 24 h after LPS treatment. miR-29b-3p overexpression or YY1 knockdown alleviated LPS-induced inflammatory responses and improved the viability of HCAECs. miR-29b-3p inhibition aggravated LPS-induced inflammatory injury in HCAECs. miR-29b-3p bound to YY1 mRNA and inhibited the expression of YY1 protein. YY1 bound to the IRAK1 promoter and activated the transcription of IRAK1. Upregulation of miR-29b-3p suppressed the inflammatory response after intraluminal injury of the common femoral artery in rats. In conclusion, dysregulation of the YY1/IRAK1 pathway via miR-29b-3p downregulation may be implicated in post-vascular injury inflammation.

Key Words: Inflammation • IRAK1 • miR-29b-3p • Percutaneous coronary intervention • YY1

INTRODUCTION

In China, cardiovascular disease (CVD) contributes to 40% of all deaths, and its epidemiology is associated with an increasing burden of atherosclerotic CVD.¹ Acute coronary syndrome (ACS) is a set of myocardial ischemic conditions that result from imbalances between oxygen supply and demand, consequently leading to unstable angina, non-ST-elevation myocardial infarction, and ST-elevation myocardial infarction.² Rupture of vulnerable atherosclerotic plaque releases thrombogenic materials into the blood and induces thrombus that provokes the

Received: April 23, 2022 Accepted: February 15, 2023

¹Department of Cardiology, Jiangxi Provincial People's Hospital, The First Affiliated Hospital of Nanchang Medical College, Nanchang, Jiangxi; ²Department of Cardiology, Union Hospital, Tongji Medical College, Huazhong University of Science and Technology, Wuhan, Hubei, P.R. China.

Corresponding author: Dr. Jianyun Lan, Department of Cardiology, Jiangxi Provincial People's Hospital, The First Affiliated Hospital of Nanchang Medical College, No. 152, Aiguo Road, Donghu District, Nanchang, Jiangxi 330000, P.R. China. E-mail: lanjianyun1980@163.com

Yunying Zhou and Yong Yang contributed equally to this research.

Abbreviations

ACS	Acute coronary syndrome
Ago2	Anti-human argonaute-2
CCK-8	Cell counting kit-8
ChIP	Chromatin immunoprecipitation
CVD	Cardiovascular disease
ELISA	Enzyme-linked immunosorbent assay
GAPDH	Glyceraldehyde 3-phosphate dehydrogenase
HCAECs	Human coronary artery endothelial cells
H&E	Hematoxylin-eosin
IA/MA	Intimal area/medial area
IgG	Immunoglobulin G
IL-1	Interleukin-1
IL-1 β	Interleukin-1beta
IL-6	Interleukin-6
IRAK1	Interleukin-1 receptor-associated kinase 1
LPS	Lipopolysaccharide
miRNAs	MicroRNAs
NC	Negative control
PCI	Percutaneous coronary intervention
qRT-PCR	Quantitative reverse transcription polymerase chain reaction
RIP	RNA immunoprecipitation
RIPA	Radioimmunoprecipitation assay
sVCAM-1	Soluble vascular cell adhesion molecule-1
TNF- α	Tumor necrosis factor- α
YY1	Yin Yang 1

ischemic characteristics of ACS.³ Percutaneous coronary intervention (PCI) has been the most common therapeutic method for managing coronary artery stenosis over the past few decades.⁴ However, the implanted stent may cause damage to the vessel wall and result in increased serum levels of inflammatory factors, which is associated with adverse cardiovascular events post PCI.⁵

MicroRNAs (miRNAs) are short RNAs of 19 to 25 nucleotides that can post-transcriptionally silence genes involved in functional interaction pathways.⁶ Mature miRNAs are guided to the 3' end of mRNAs through base pairing, which induces subsequent gene silencing by destabilizing or translationally repressing the target mRNA.⁷ A previous study reported a decrease in the expression of plasma miR-126 in ACS patients at 72 h post PCI, which was correlated with increases in the expression of the inflammatory markers high-sensitive C-reactive protein and vascular cell adhesion molecule-1 (VCAM-1).⁸ To date, there is scarce evidence regarding the involvement

of miRNAs in PCI-induced short-term inflammation. miR-29b-3p has been reported to be upregulated in myocardial ischemia/reperfusion injury after PM2.5 exposure and to promote myocardial inflammation and apoptosis by regulating the phosphoinositide 3-kinase pathway.⁹ However, it is unknown whether miR-29b-3p regulates cardiac inflammatory responses following PCI.

Interleukin (IL)-1 receptor-associated kinases (IRAKs) are intracellular kinases participating in Toll-like receptor and IL-1 signaling pathways that regulate immune and inflammatory responses.¹⁰ The overexpression of miR-142-3p has been shown to alleviate myocardial injury and inflammation following coronary microembolization (a common complication of PCI) partially by inhibiting the expression of IRAK1; moreover, a lower plasma level of miR-142-3p has been reported in ACS patients with no-reflow after primary PCI.¹¹ These findings show that IRAK1 is a potential regulator of post-PCI inflammatory responses. A previous study found that IL-1 β increased the abundance of transcription factor Yin Yang 1 (YY1) in cardiac myocytes and also induced YY1 phosphorylation to enhance the DNA binding activity of YY1,¹² suggesting a positive correlation between YY1 and IRAK1. Moreover, YY1 has been identified as a target of miR-29b in angiotensin II-stimulated muscle atrophy.¹³ Therefore, we speculated that miR-29b-3p might regulate inflammatory responses via YY1/IRAK1.

ACS is characterized by vascular inflammation during which endothelial cells enhance the attachment and migration of immune cells to the arterial wall via up-regulated adhesion molecules.¹⁴ In this study, we measured the serum levels of soluble VCAM-1 (sVCAM-1) and inflammatory cytokines in ACS patients after PCI. The function and action mechanism of miR-29b-3p in post-vascular injury inflammation were studied in inflammatory human coronary artery endothelial cells (HCAECs) *in vitro* and in a rat model of intraluminal injury of the common femoral artery.

MATERIALS AND METHODS

Clinical samples

This study involved 85 patients with ACS who planned to undergo PCI (34 males and 51 females with an average age of 65.14 ± 4.12 years) and 50 control patients with

normal coronary arteries (24 males and 26 females with an average age of 64.14 ± 5.52 years) at a local hospital. All ACS patients were diagnosed with acute myocardial infarction by coronary angiography and showed no significant differences in gender and age ($p > 0.05$). Patients with cardiomyopathy, autoimmune diseases, diabetes, severe infections, malignant tumors or severe liver/kidney dysfunction were excluded from this study. Blood samples were collected and used under the approval of the ethics committee of the local hospital and after written informed consent had been obtained from all patients or their families.

Cell culture

HCAECs were purchased from the American Type Culture Collection (Manassas, VA, USA) and cultured in 10% fetal bovine serum-Dulbecco's modified Eagle medium (Thermo Fisher Scientific, Wilmington, DE, USA) with 5% CO₂ at 37 °C. Adherent cells were subcultured and dissociated with 0.25% trypsin (HyClone, Logan, UT, USA). Cells in the logarithmic growth phase were harvested for experiments.

Cell transfection

miR-29b-3p mimic (50 nM), miR-29b-3p inhibitor (100 nM), YY1 shRNA (sh-YY1; 2 µg), IRAK1 overexpression vector (oe-IRAK1; 2 µg), and negative controls (mimic NC, inhibitor NC, sh-NC, and oe-NC) (GenePharma, Shanghai, China) were delivered by Lipofectamine 2000 reagent (Invitrogen, Carlsbad, CA, USA) into HCAECs 48 h before other *in vitro* experiments.

Cell counting kit-8 (CCK-8) assay

HCAECs in the logarithmic growth phase were seeded at 1×10^4 cells per well in a 96-well plate and precultured for 24 h before transfection. Forty-eight hours after transfection, the cells were incubated with 10 µL of CCK-8 reagent (CK04; Dojindo, Kumamoto, Japan) at 37 °C for 3 h. Absorbance at 450 nm was measured by a microplate reader.

Quantitative reverse transcription polymerase chain reaction (qRT-PCR)

TRIzol reagent (Invitrogen, Carlsbad, CA, USA) was used for isolation of total RNA. cDNA was synthesized using reverse transcription kits (Takara, Tokyo, Japan) and mixed with SYBR Green Mix (Roche Diagnostics, India-

napolis, IN, USA). The cDNA (3 duplicates per sample) was amplified by thermal cycling (10 s, 95 °C; 45 cycles of 5 s at 95 °C, 10 s at 60 °C, and 10 s at 72 °C; 5 min, 72 °C) on a LightCycler 480 Instrument (Roche Diagnostics). Relative expression changes of target genes were analyzed by the $2^{-\Delta\Delta Ct}$ method. Primers of target genes and reference genes (glyceraldehyde 3-phosphate dehydrogenase [GAPDH] and U6) are shown in Table 1.

Western blotting

Total protein was isolated from samples lysed with radioimmunoprecipitation assay (RIPA) buffer (Beyotime, Shanghai, China) and quantified using bicinchoninic acid kits (Beyotime). Proteins were mixed with loading buffer (Beyotime) and heated in boiling water for 3 min. Protein electrophoresis was started at 80 V for 30 min and continued at 120 V for 1-2 h after bromophenol blue reached the separation gel. Separated proteins were transferred onto a membrane in an ice bath at 300 mA for 60 min. The membrane was rinsed for 1-2 min and immersed in blocking buffer at room temperature for 60 min. After that, the membrane was incubated with antibodies against GAPDH (5174S, 1:1000; Cell Signaling Technology, Danvers, MA, USA), YY1 (ab109237, 1:1000; Abcam, Cambridge, MA, USA), IRAK1 (ab180747, 1:1000; Abcam), IL-1β (ab254360, 1:1000; Abcam), IL-6 (ab9324, 1:1000; Abcam), and tumor necrosis factor (TNF)-α (ab205587, 1:1000; Abcam) on a shaking bed at room temperature for 60 min. After rinsing (3 × 10 min), the membrane was subjected to 60 min of incubation with secondary antibody (horseradish peroxidase-labelled goat anti rabbit immunoglobulin G [IgG], 1:5000; Com-

Table 1. Primer sequences

Name of primer	Sequences (5'-3')
miR-29b-3p-F	ACACTCCAGCTGGGTAGCACCATTTC
miR-29b-3p-R	TGGTGTCTGGAGATCG
U6-F	CTCTCGCTTCGGCAGCAC
U6-R	ACGCTTCACGAATTTGCGT
IRAK1-F	CAGTTCGCCGCCCTGAT
IRAK1-R	CTGGAAAAGCTGGGGAGAGG
YY1-F	TCAGACAAGTCACGTCAGGC
YY1-R	CTCCATGTGTACCTCCAC
GAPDH-F	ACTAGGCGCTCACTGTTCTC
GAPDH-R	TCGCCCACTTGATTTTGA

F, forward; GAPDH, glyceraldehyde 3-phosphate dehydrogenase; IRAK1, Interleukin-1 receptor-associated kinase 1; miR, microRNA; R, reverse; U6, small nuclear RNA U6; YY1, Yin Yang 1.

Win Biotech, Beijing, China) at room temperature. Protein expression was visualized with color developing solution and detected by a chemiluminescence imaging system (Bio-Rad, Hercules, CA, USA).

Dual-luciferase reporter assay

The StarBase database (<http://starbase.sysu.edu.cn/>) was used to predict the binding sites between YY1 and miR-29b-3p. Wild-type and mutant binding sequences of YY1 (WT-YY1 and MUT-YY1) were synthesized and separately inserted into pGL3-Promoter vectors (Promega, Madison, WI, USA). The vectors together with miR-29b-3p mimic (30 nM) or mimic NC (30 nM) were delivered into HEK293T cells (Shanghai Sixin Biotechnology Co., Ltd., Shanghai, China). The JASPAR database (<http://jaspar.genereg.net/>) was used to predict the binding sites between YY1 and IRAK1. Wild-type and mutant sequences (WT-IRAK1 and MUT-IRAK1) of the predicted YY1-binding site on IRAK1 promoter were separately cloned into pGL3-Basic vectors (Promega) and cotransfected with YY1 overexpression plasmids or corresponding NC into HEK293T cells. The activity of Firefly luciferase and Renilla luciferase (internal control) was measured by a fluorescence detector (Promega). This assay was independently repeated three times.

RNA immunoprecipitation (RIP)

A RIP kit (Millipore, Burlington, MA, USA) was used for this assay. HCAECs were washed with precooled phosphate-buffered saline and lysed with an equal volume of RIPA buffer (P0013B; Beyotime) in an ice bath for 5 min. The lysate was centrifuged at 14,000 rpm at 4 °C for 10 min. One part of the supernatant was taken as the input and the other was incubated with antibodies. Magnetic beads (50 µL) were washed, resuspended in 100 µL of RIP Wash Buffer, and incubated with 5 µg of rabbit anti-human argonaute-2 (Ago2) (1:50, ab186733, Abcam, Cambridge, MA, USA) or IgG (1:100, ab172730, Abcam) at room temperature for 30 min. The bead-antibody complex was washed, resuspended in 900 µL of RIP Wash Buffer, and incubated with 100 µL of the supernatant at 4 °C overnight. The complex was washed 3 times and collected on a magnetic grate.

Chromatin immunoprecipitation (ChIP)

HCAECs were treated with 1% formaldehyde for

DNA-protein crosslinking. Extracted DNA was sonicated into 200-1000 bp fragments and incubated with 60 µL of Protein G magnetic beads at 4 °C (1 h) to remove non-specific antibodies. The mixture was centrifuged at 6,500 rpm for 1 min. Supernatant was incubated with 4 µg of YY1 antibody or normal rabbit IgG antibody on a shaker at 4 °C overnight. The antibody-chromatin complex was incubated with 60 µL of Protein G magnetic beads at 4 °C for 1 h and centrifuged at 6,500 rpm for 1 min. The bead complex was incubated with 100 µL of eluant at room temperature for 15 min and centrifuged at 6,500 rpm for 1 min. Supernatant was transferred into an empty centrifuge tube and reached a total amount of 200 µg before de-crosslinking and DNA purification. DNA precipitated by YY1 antibody was used as a template to amplify the predicted YY1-binding site of IRAK1 promoter. A ChIP analysis kit (Wanlei Biotech Co., Ltd., Shenyang, China) was used for this assay. IRAK1-forward primer: CTCCTGGTAACAGCCCTGC; IRAK1-reverse primer: GACTC ACTTCCCTTCGAGC (350 bp).

Enzyme-linked immunosorbent assay (ELISA)

Serum was separated from 2 ml of blood by centrifugation and refrigerated in aliquots at -20 °C. ELISA kits (R&D Systems, Minneapolis, MN, US) were used to measure the concentrations of sVCAM-1, IL-1β, IL-6, and TNF-α in serum and cell culture supernatant.

Wire-induced femoral artery injury

The animal experiments were performed in strict accordance with the guidelines of the Institutional Animal Care and Use Committee of the local hospital. Male Wistar rats (8 weeks old) from Beijing Huafukang Biotechnology Co., Ltd. (Beijing, China) were housed in a standard laboratory environment (21 ± 1 °C; 45-55% humidity; 12 h light/12 h dark) with free access to food and water. The rats were randomly divided into 3 groups (n = 6 per group): sham group (sham-operated), injury group (with intraluminal injury of the common femoral artery), and miR-29b-3p agomir group (given tail vein injection of miR-29b-3p agomir [GenePharma] 3 days before modeling).

The intraluminal injury of the common femoral artery was caused by three passages of an angioplasty guide wire with a diameter of 0.25 mm (Advanced Cardiovascular Systems, Santa Clara, CA, USA) as previously described.¹⁵ A groin incision was made, and the femoral ar-

tery was temporarily clamped at the level of the inguinal ligament. An arteriotomy was performed on the profunda branch, and the guidewire was inserted. The clamp was removed, and the wire was pushed to the aortic bifurcation and pulled back. After removal of the wire, the arteriotomy site was ligated. The arteries of the rats from the sham group were separated, temporarily clamped, opened, and ligated, without any passages of wires. The rats were sacrificed 7 days later, and the femoral arteries were collected (some were cryopreserved at -80°C for qRT-PCR and western blotting, and the others were paraffin-embedded for hematoxylin-eosin [H&E] staining).

H&E staining

H&E staining was used to evaluate vascular morphological changes. Femoral artery tissues were fixed and embedded in paraffin. Paraffin-embedded tissues were transverse-sectioned into $5\text{ }\mu\text{m}$ slices and then stained with H&E (Solarbio, Beijing, China) based on standard protocols. The stained sections were observed under an OLYMPUS BX53 light microscope (Tokyo, Japan). The structure of the artery wall was divided by the inner and outer elastic membranes. The H&E-stained images were imported into Image-Pro plus 5.0 image analysis software. The outer and inner elastic membranes and the lumen were accurately outlined with a mouse. Intimal and lumen areas were measured and intimal area/medial area (IA/MA) ratios were calculated to reveal the severity of intimal hyperplasia.

Statistical analysis

Data were analyzed by GraphPad Prism 7.0 and presented as mean \pm standard deviation. The cell experiments were repeated thrice. The t test was used to compare differences between two sets of data. One-way analysis of variance was used to compare differences among multiple groups. Tukey's test was used for post hoc multiple comparisons. Differences were considered significant if $p < 0.05$.

RESULTS

Low expression of plasma miR-29b-3p one day after PCI

The 85 patients with ACS and 50 healthy controls

with normal coronary arteries underwent fasting blood tests. For each participant, 10 ml of cubital venous blood was taken each time. The ACS patients were sampled before PCI, 1 day after PCI, and 30 days after PCI. The PCR tests showed that the expression of plasma miR-29b-3p was reduced 1 day after PCI compared to the expression before PCI (Figure 1, $p < 0.05$). Moreover, the results of ELISA showed that the serum levels of sVCAM-1, IL-1 β , IL-6, and TNF- α were increased 1 day after PCI compared to the levels before PCI (Table 2, $p < 0.05$). There were no significant differences in the expression of plasma miR-29b-3p or the serum levels of sVCAM-1, IL-1 β , IL-6, and TNF- α between the patients sampled 30 days after PCI and controls. These results indicated that the levels of miR-29b-3p and inflammatory molecules were significantly affected on the first day after PCI and returned to normal 30 days after PCI.

HCAEC model of inflammatory injury

To explore the function and action mechanism of miR-29b-3p in post-vascular injury inflammation, we treated HCAECs with $1\text{ }\mu\text{g/ml}$ lipopolysaccharide (LPS) for 24 h to establish an inflammatory injury model. LPS treatment reduced the expression of miR-29b-3p in HCAECs (Figure 2A, $p < 0.05$), increased the levels of

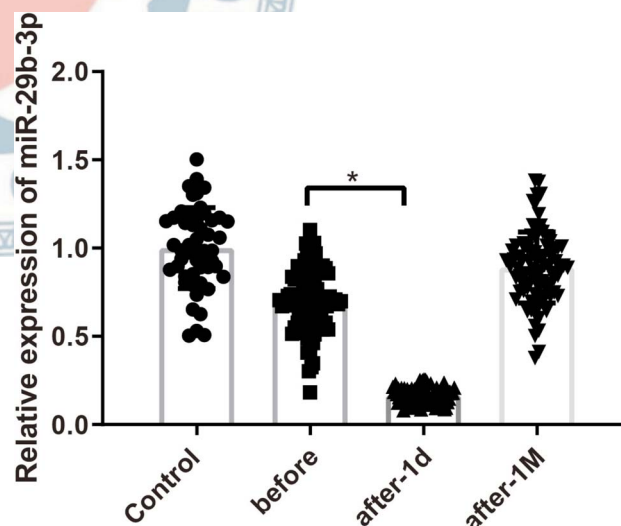


Figure 1. Low expression of plasma microRNA (miR)-29b-3p one day after percutaneous coronary intervention (PCI). Note: Quantitative reverse transcription polymerase chain reaction (qRT-PCR) was used to detect the expression of plasma miR-29b-3p before PCI, 1 day after PCI, and 30 days after PCI. The data were expressed as mean \pm standard deviation. Two groups were compared by student's t-test. * $p < 0.05$, compared with the before group.

Table 2. Enzyme-linked immunosorbent assay for detecting sVCAM-1, IL-1 β , IL-6, and TNF- α in patient serum

Group	sVCAM-1 (ng/L)	IL-1 β (ng/L)	IL-6 (ng/L)	TNF- α (ng/L)
Before	428.49 \pm 17.74	26.37 \pm 3.21	152.33 \pm 21.89	23.16 \pm 1.32
After-1d	564.28 \pm 22.13*	37.22 \pm 2.65*	245.97 \pm 31.64*	38.32 \pm 2.01*
After-30d	397.17 \pm 18.32	19.52 \pm 3.01	90.87 \pm 26.86	16.15 \pm 1.82
Control	378.35 \pm 15.54	18.32 \pm 2.32	99.43 \pm 32.11	15.65 \pm 2.17

Note: The data were expressed as mean \pm standard deviation. Differences between two groups were compared by student's t-test.

* $p < 0.05$, compared with the before group.

IL, interleukin; sVCAM-1, soluble vascular cell adhesion molecule-1; TNF, tumor necrosis factor.

sVCAM-1, IL-1 β , IL-6, and TNF- α in culture supernatant (Table 3, $p < 0.05$), and impaired the viability of HCAECs (Figure 2B, $p < 0.05$). These data were consistent with the clinical findings and indicated successful establishment of a cellular model of inflammatory injury.

Overexpression of miR-29b-3p downregulated YY1 and reduced HCAEC inflammation

miR-29b-3p was predicted by StarBase to have binding sites for YY1 mRNA (Figure 3A). Compared with the transfection of mimic NC, the transfection of miR-29b-3p

mimic together with YY1-WT instead of YY1-MUT significantly reduced relative luciferase activity in the dual-luciferase reporter assay (Figure 3B, $p < 0.05$). Compared with IgG antibody, Ago2 antibody significantly pulled down miR-29b-3p and YY1 mRNA (Figure 3C, $p < 0.05$). The results of these two experiments validated the binding relationship between miR-29b-3p and YY1 mRNA.

We transfected LPS-treated HCAECs with miR-29b-3p mimic, mimic NC, miR-29b-3p inhibitor or inhibitor NC to investigate the effect of miR-29b-3p expression on HCAEC inflammation. The expression of miR-29b-3p was successfully promoted or inhibited in HCAECs (Figure 3D, $p < 0.05$). The overexpression of miR-29b-3p downregulated YY1 and IRAK1, while inhibition of miR-29b-3p upregulated these two proteins in HCAECs (Figure 3E-F, $p < 0.05$). Moreover, the levels of sVCAM-1, IL-1 β , IL-6, and TNF- α were reduced (Table 4, $p < 0.05$) and the viability of HCAECs was enhanced (Figure 3G, $p < 0.05$) in the presence of miR-29b-3p mimic; opposite results were observed in the presence of miR-29b-3p inhibitor.

YY1 stimulated HCAEC inflammation by promoting IRAK1 transcription

Information on the University of California Santa Cruz database showed that YY1 was a transcription factor of IRAK1 (Figure 4A). YY1 was predicted by JASPAR to have binding sites for IRAK1 promoter (Figure 4B). Compared

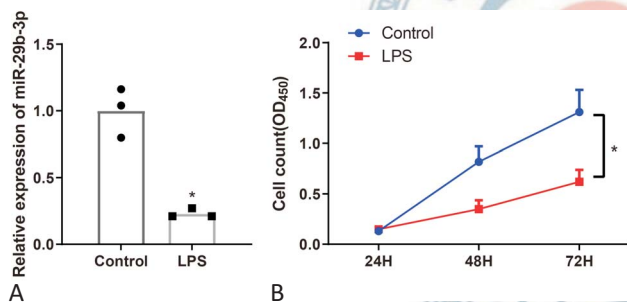


Figure 2. Human coronary artery endothelial cell (HCAEC) model of inflammatory injury. Note: HCAECs were treated with 1 μ g/ml lipopolysaccharide (LPS) for 24 h. (A) Quantitative reverse transcription polymerase chain reaction (qRT-PCR) was used to detect the expression of microRNA-29b-3p in HCAECs. (B) Cell counting kit-8 (CCK-8) was used to detect the viability of HCAECs. The data were expressed as mean \pm standard deviation. The two groups of data were compared by student's t-test. Each experiment was repeated 3 times. * $p < 0.05$, compared with the control group.

Table 3. Enzyme-linked immunosorbent assay for detecting sVCAM-1, IL-1 β , IL-6, and TNF- α in cell culture supernatant

Group	sVCAM-1 (ng/L)	IL-1 β (ng/L)	IL-6 (ng/L)	TNF- α (ng/L)
Control	341.65 \pm 13.33	18.87 \pm 2.80	101.62 \pm 22.78	16.09 \pm 3.09
LPS	483.83 \pm 15.53*	35.28 \pm 3.12*	230.04 \pm 29.01*	32.64 \pm 2.87*

Note: Human coronary artery endothelial cells were treated with 1 μ g/ml LPS for 24 h. The data were expressed as mean \pm standard deviation. Differences between two groups were compared by student's t-test. * $p < 0.05$, compared with the control group.

IL, interleukin; LPS, lipopolysaccharide; sVCAM-1, soluble vascular cell adhesion molecule-1; TNF, tumor necrosis factor.

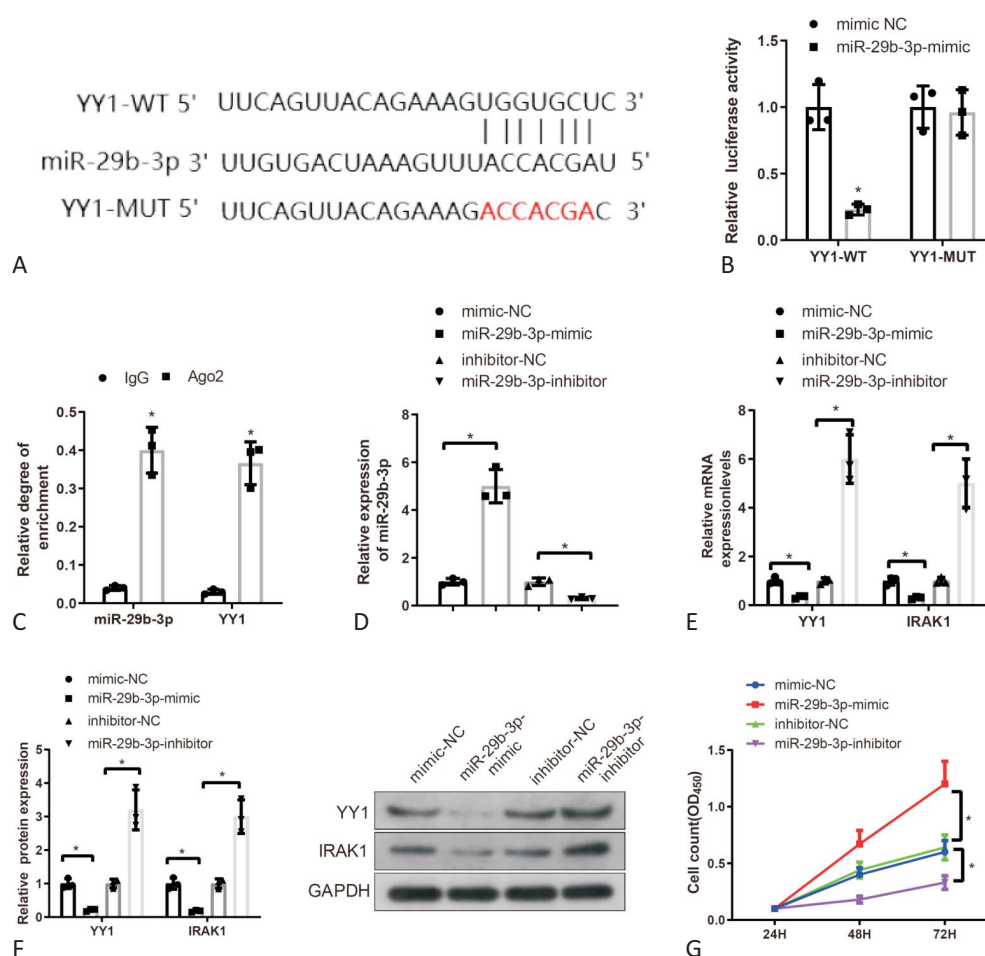


Figure 3. Overexpression of microRNA (miR)-29b-3p downregulates Yin Yang 1 (YY1) and reduces human coronary artery endothelial cell (HCAEC) inflammation. Note: (A) StarBase predicted the binding sites between microRNA (miR)-29b-3p and YY1. (B) Dual-luciferase reporter assay was performed to verify the binding relationship between miR-29b-3p and YY1. (C) RNA immunoprecipitation (RIP): quantitative reverse transcription polymerase chain reaction (qRT-PCR) was used to detect the levels of miR-29b-3p and YY1 mRNA in the complexes pulled down by anti-immunoglobulin G (IgG) and anti-argonaute-2 antibodies. HCAECs were treated with lipopolysaccharide and transfected with miR-29b-3p mimic, mimic negative control (NC), miR-29b-3p inhibitor or inhibitor NC. (D-E) qRT-PCR was used to detect the expression of miR-29b-3p (D), YY1 and interleukin-1 receptor-associated kinase 1 (IRAK1) (E) in HCAECs; (F) western blotting was used to detect YY1 and IRAK1 proteins in HCAECs; (G) cell counting kit-8 (CCK-8) was used to detect the viability of HCAECs. The data were expressed as mean \pm standard deviation. Two groups were compared by student's t-test. Each experiment was repeated 3 times. * $p < 0.05$, compared with the IgG, mimic NC or inhibitor NC group.

Table 4. Enzyme-linked immunosorbent assay for detecting sVCAM-1, IL-1 β , IL-6, and TNF- α in cell culture supernatant

Group	sVCAM-1 (ng/L)	IL-1 β (ng/L)	IL-6 (ng/L)	TNF- α (ng/L)
Mimic NC	491.55 \pm 21.11	33.76 \pm 2.99	228.33 \pm 27.12	30.96 \pm 1.43
miR-29b-3p mimic	323.89 \pm 20.32*	17.54 \pm 2.95*	96.97 \pm 28.47*	15.32 \pm 1.65*
Inhibitor NC	501.43 \pm 20.29	32.65 \pm 2.53	232.87 \pm 25.32	31.15 \pm 1.33
miR-29b-3p inhibitor	622.49 \pm 18.94 [#]	48.23 \pm 3.16 [#]	312.43 \pm 29.19 [#]	43.65 \pm 2.01 [#]

Note: Human coronary artery endothelial cells were treated with lipopolysaccharide and transfected with miR-29b-3p mimic, mimic NC, miR-29b-3p inhibitor or inhibitor NC. The data were expressed as mean \pm standard deviation. Differences between two groups were compared by student's t-test. * $p < 0.05$, compared with the mimic NC group; [#] $p < 0.05$, compared with the inhibitor NC group.

IL, interleukin; miR, microRNA; NC, negative control; sVCAM-1, soluble vascular cell adhesion molecule-1; TNF, tumor necrosis factor.

with the transfection of empty vectors, the transfection of YY1 overexpression plasmids together with IRAK1-WT instead of IRAK1-MUT significantly increased relative luciferase activity in the dual-luciferase reporter assay (Figure 4C, $p < 0.05$). The results of ChIP assay showed that YY1 antibody pulled down IRAK1 promoter in HCAECs (Figure 4D, $p < 0.05$). The results of these two experiments validated the binding relationship between YY1 and IRAK1 promoter. YY1 was knocked down by shRNA in HCAECs (Figure 4E-F, $p < 0.05$). Knockdown of YY1 inhibited the levels of IRAK1 mRNA and protein (Figure 4E-F, $p < 0.05$), reduced the levels of sVCAM-1, IL-1 β , IL-6, and TNF- α (Table 5, $p < 0.05$), and promoted the viability of HCAECs (Figure

4G, $p < 0.05$).

miR-29b-3p regulated HCAEC inflammation via the YY1/IRAK1 axis

To ascertain regulation of the YY1/IRAK1 axis by miR-29b-3p in LPS-stimulated inflammatory response of HCAECs, we delivered miR-29b-3p mimic together with oe-IRAK1 into LPS-treated HCAECs. Compared with the miR-29b-3p mimic + oe-NC group, the miR-29b-3p mimic + oe-IRAK1 group exhibited increases in the levels of IRAK1 mRNA and protein, but there were no significant differences in the expression of miR-29b-3p and YY1 (Figure 5A-B, $p < 0.05$). More importantly, the miR-29b-3p mimic + oe-IRAK1 group showed higher levels of sVCAM1, IL-1 β ,

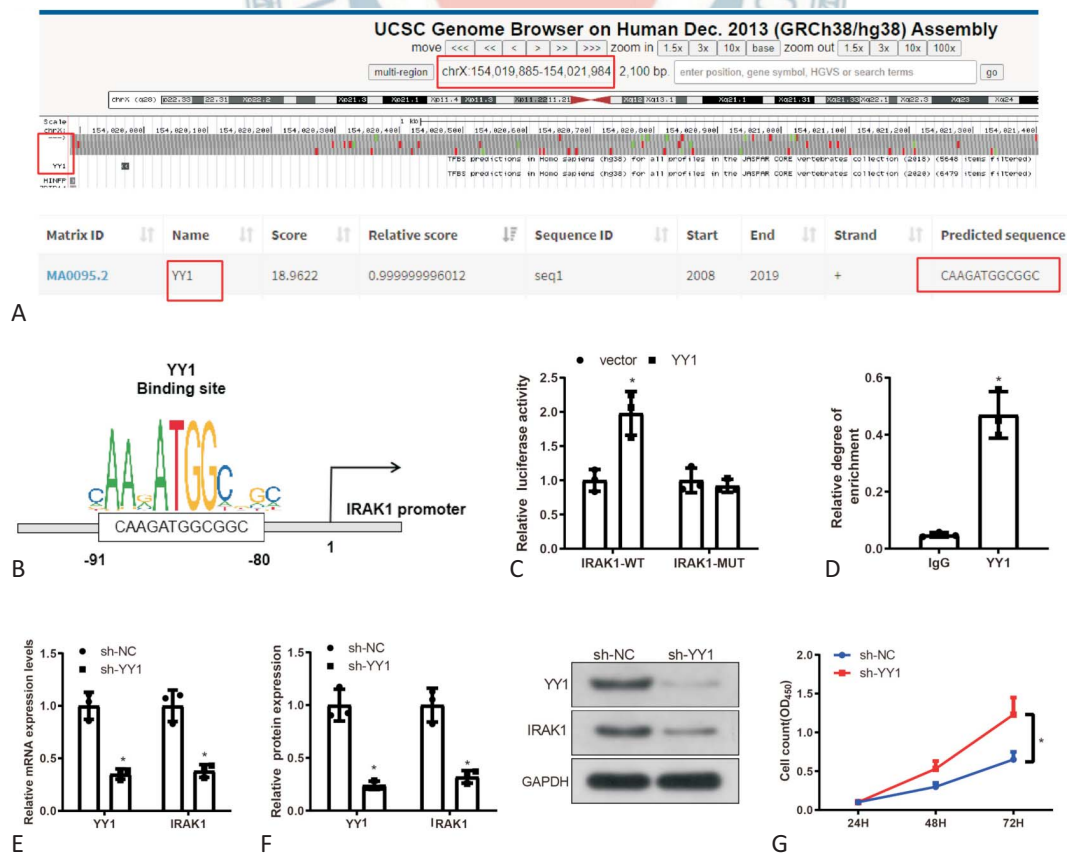


Figure 4. Yin Yang 1 (YY1) stimulates human coronary artery endothelial cell (HCAEC) inflammation by promoting interleukin-1 receptor-associated kinase 1 (IRAK1) transcription. Note: (A) YY1 was predicted by the University of California Santa Cruz database to be a transcription factor of IRAK1. (B) JASPAR predicted the binding sites between YY1 and IRAK1 promoter. Dual-luciferase reporter assay (C) and chromatin immunoprecipitation (ChIP) (D) were performed to verify the binding relationship between YY1 and IRAK1 promoter. HCAECs were treated with lipopolysaccharide and transfected with shRNA negative control (sh-NC) or shRNA targeting YY1 (sh-YY1): (E) Quantitative reverse transcription polymerase chain reaction (qRT-PCR) was used to detect the expression of YY1 mRNA and IRAK1 mRNA in HCAECs; (F) western blotting was used to detect YY1 and IRAK1 proteins in HCAECs; (G) cell counting kit-8 (CCK-8) was used to detect the viability of HCAECs. The data were expressed as mean \pm standard deviation. Two groups were compared by student's t-test. Each experiment was repeated 3 times. * $p < 0.05$, compared with the vector, immunoglobulin G (IgG), or sh-NC group.

Table 5. Enzyme-linked immunosorbent assay for detecting sVCAM-1, IL-1 β , IL-6, and TNF- α in cell culture supernatant

Group	sVCAM-1 (ng/L)	IL-1 β (ng/L)	IL-6 (ng/L)	TNF- α (ng/L)
sh-NC	474.86 \pm 11.65	33.73 \pm 1.89	222.86 \pm 12.80	30.65 \pm 2.21
sh-YY1	310.78 \pm 10.13*	16.92 \pm 1.31*	87.43 \pm 12.42*	15.28 \pm 1.89*

Note: Human coronary artery endothelial cells were treated with lipopolysaccharide and transfected with sh-NC or sh-YY1. The data were expressed as mean \pm standard deviation. Differences between two groups were compared by student's t-test. * $p < 0.05$, compared with the sh-NC group.

IL, interleukin; NC, negative control; sh, shRNA; sVCAM-1, soluble vascular cell adhesion molecule-1; TNF, tumor necrosis factor.

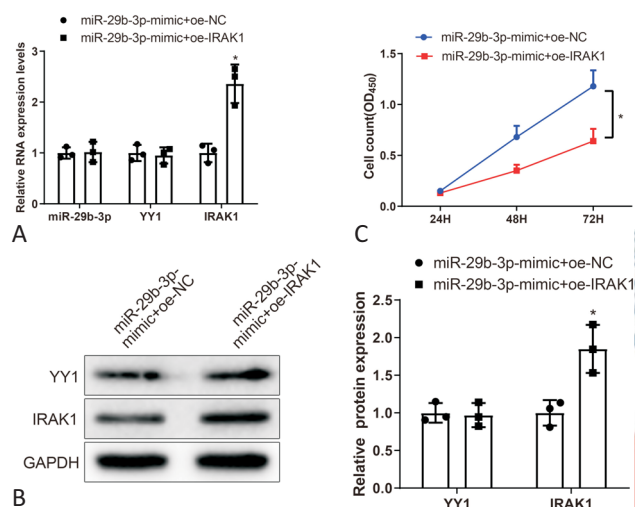


Figure 5. MicroRNA (miR)-29b-3p mitigates human coronary artery endothelial cell (HCAEC) inflammation via the Yin Yang 1 (YY1)/interleukin-1 receptor-associated kinase 1 (IRAK1) axis. Note: Lipopolysaccharide-treated HCAECs were transfected with miR-29b-3p mimic + negative control overexpression vector (oe-NC) or miR-29b-3p mimic + IRAK1 overexpression vector (oe-IRAK1). (A) Quantitative reverse transcription polymerase chain reaction (qRT-PCR) was used to detect the expression of miR-29b-3p, YY1 mRNA, and IRAK1 mRNA in HCAECs; (B) western blotting was used to detect YY1 and IRAK1 proteins in HCAECs; (C) cell counting kit-8 (CCK-8) was used to detect the viability of HCAECs. The data were expressed as mean \pm standard deviation. The two groups of data were compared by student's t-test. Each experiment was repeated 3 times. * $p < 0.05$, compared with the miR-29b-3p mimic + oe-NC group. GAPDH, glyceraldehyde 3-phosphate dehydroge.

IL-6, and TNF- α (Table 6) and lower cell viability (Figure 5C, $p < 0.05$) than the miR-29b-3p mimic + oe-NC group, indicating that miR-29b-3p reduced the inflammatory response of HCAECs through the YY1/IRAK1 axis.

Upregulation of miR-29b-3p suppressed the inflammatory response after intraluminal injury of the common femoral artery in rats

We then tested the role of miR-29b-3p and relevant mechanisms within endothelial cells in a rat model of wire-induced femoral artery injury. miR-29b-3p was down-regulated and YY1 and IRAK1 were upregulated in the femoral artery tissues of rats with wire injury; miR-29b-3p agomir treatment increased the expression of miR-29b-3p and decreased the expression levels of YY1 and IRAK1 in injured rats (Figure 6A-B, $p < 0.05$). The intima was thickened with an increased IA/MA ratio and the lumen area was narrowed in rats with wire injury, which was ameliorated by the upregulation of miR-29b-3p (Figure 6C, $p < 0.05$). Western blot experiments also showed that the levels of IL-1 β , IL-6, and TNF- α were increased in the femoral artery tissues of rats with wire injury; however, the levels of the inflammatory factors were suppressed by upregulation of miR-29b-3p (Figure 6D, $p < 0.05$).

Table 6. Enzyme-linked immunosorbent assay for detecting sVCAM-1, IL-1 β , IL-6, and TNF- α in cell culture supernatant

Group	sVCAM-1 (ng/L)	IL-1 β (ng/L)	IL-6 (ng/L)	TNF- α (ng/L)
miR-29b-3p mimic + oe-NC	344.86 \pm 8.16	15.53 \pm 1.74	98.06 \pm 11.42	13.95 \pm 3.01
miR-29b-3p mimic + oe-IRAK1	460.78 \pm 10.13*	26.88 \pm 1.41*	217.73 \pm 11.81*	29.06 \pm 1.47*

Note: Human coronary artery endothelial cells were treated with lipopolysaccharide and transfected with miR-29b-3p mimic + oe-NC or miR-29b-3p mimic + oe-IRAK1. The data were expressed as mean \pm standard deviation. Differences between two groups were compared by student's t-test. * $p < 0.05$, compared with the miR-29b-3p mimic + oe-NC group.

IL, interleukin; miR, microRNA; NC, negative control; oe, overexpression; sVCAM-1, soluble vascular cell adhesion molecule-1; TNF, tumor necrosis factor.

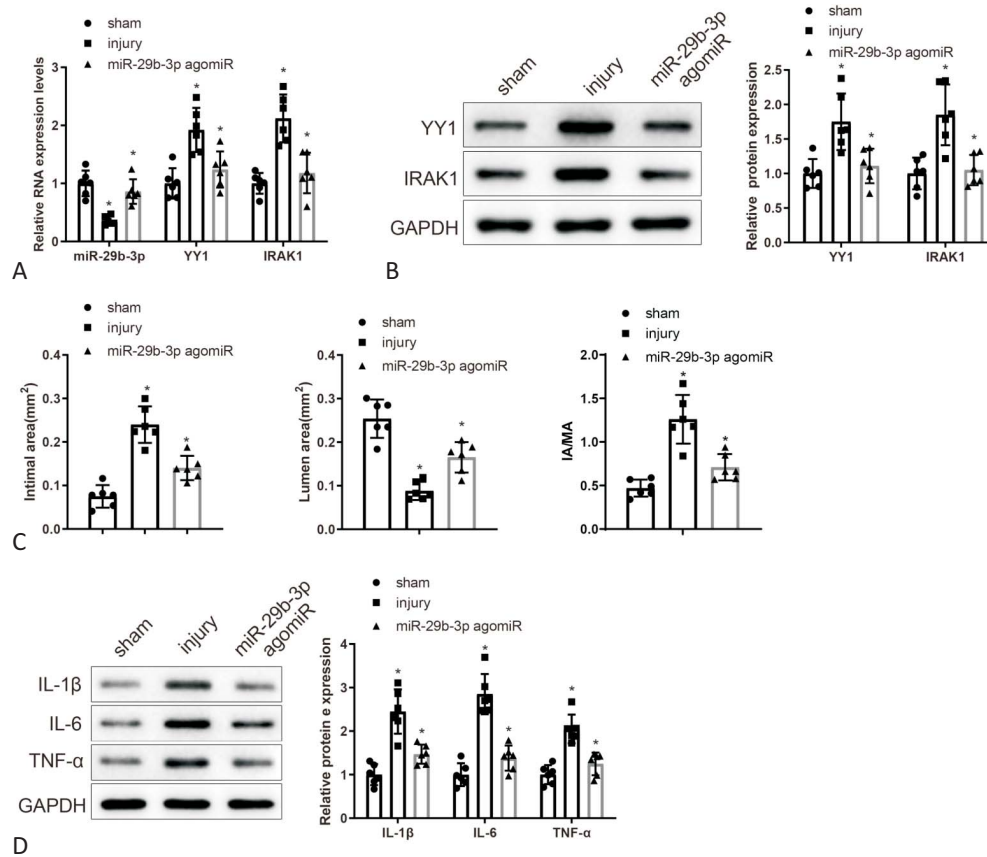


Figure 6. Upregulation of microRNA (miR)-29b-3p suppresses inflammatory response after intraluminal injury of the common femoral artery in rats. Note: (A) Quantitative reverse transcription polymerase chain reaction (qRT-PCR) was used to detect the expression of miR-29b-3p, Yin Yang 1 (YY1) mRNA, and interleukin (IL)-1 receptor-associated kinase 1 (IRAK1) mRNA in femoral artery tissues; (B) western blotting was used to detect YY1 and IRAK1 proteins in femoral artery tissues; (C) the intimal and lumen areas of femoral arteries and the intimal area/medial area ratios; (D) western blotting was used to detect IL-1 β , IL-6, and tumor necrosis factor- α in femoral artery tissues. Each group had 6 rats. The data were expressed as mean \pm standard deviation. One-way analysis of variance was used for the group comparisons, followed by Tukey's multiple comparisons test. * $p < 0.05$, compared with the sham or injury group. GAPDH, glyceraldehyde 3-phosphate dehydrogenase; TNF, tumor necrosis factor.

DISCUSSION

PCI is applied in approximately 60% of patients with ACS and reduces myocardial infarction and deaths.¹⁶ Despite advances in devices and technologies, PCI is associated with adverse periprocedural events such as coronary perforation, abrupt vessel closure, device embolization, stent deformation and rotational atherectomy burr entrapment that can, in some cases, lead to hemodynamic compromise or even death.¹⁷ Vascular inflammation plays a central role in response to vascular injury after PCI and is linked to subsequent adverse clinical events.¹⁸ Timely management of vascular inflammation is essential for improving post-PCI outcomes. The findings of this study indicate that the overexpression of

miR-29b-3p can reduce LPS-induced inflammatory responses of HCAECs and inflammation post wire-induced femoral artery injury by inhibiting the YY1-dependent transcription of IRAK1.

In this study, we first measured the expression of plasma miR-29b-3p and the serum levels of sVCAM-1, IL-1 β , IL-6, and TNF- α in ACS patients before surgery, 1 day after and 30 days after PCI. The expression of plasma miR-29b-3p was decreased and the serum levels of these inflammatory factors were increased 1 day after PCI. A cellular model of inflammatory injury was established by treating HCAECs with LPS for 24 h. LPS is a major component of the outer surface of Gram-negative bacteria and a potent activator of cells in the immune and inflammatory systems, including endothelial cells.

Atherosclerosis is an inflammatory arterial disease involving endothelial cells, and it can be caused by chronic or recurring low LPS.¹⁹ LPS-stimulated HCAECs may act as inflammatory cells, thereby directly promoting the progression of congestive heart failure and coronary artery disease.²⁰ Since there is no established cellular model simulating post-PCI inflammation, we chose to explore the relationship between miR-29b-3p and inflammation in a LPS-induced cellular model. The expression of miR-29b-3p was inhibited in LPS-treated HCAECs as expected. The overexpression of miR-29b-3p reduced the secretion of sVCAM-1, IL-1 β , IL-6, and TNF- α and enhanced the viability of LPS-treated HCAECs. Inhibition of miR-29b-3p caused adverse experiment results.

Studies in recent years have shown that miR-29b-3p is a vascular regulator. The overexpression of miR-29b-3p has been shown to inhibit the osteogenic differentiation of vascular smooth muscle cells and alleviate vascular calcification by directly reducing the expression of matrix metalloproteinase 2.^{21,22} Moreover, the overexpression of miR-29b-3p has been shown to suppress the viability and mobility of human umbilical artery smooth muscle cells by targeting cell division cycle 7-related protein kinase.²³ The downregulation of miR-29b-3p has also been found in coronary sinus blood of patients with heart failure and to be correlated with elevated left ventricular filling pressure.²⁴ Transcoronary concentration gradients of miR-29b-3p have been significantly correlated with overall atherosclerotic plaque burden and shown predictive value for thin-cap fibroatheromas.²⁵ miR-29b-3p has exhibited regulatory effects on osteoarthritis,²⁶ ischemic inflammation,²⁷ and particulate matter-induced inflammatory response,²⁸ but its role in vascular inflammation is as yet poorly understood.

In the present study, the overexpression of miR-29b-3p reduced the expression of YY1 and IRAK1 in LPS-treated HCAECs, and the mRNA of YY1 was demonstrated to have binding sites for miR-29b-3p. Knockdown of YY1 suppressed the secretion of sVCAM-1, IL-1 β , IL-6, and TNF- α and strengthened the viability of LPS-treated HCAECs. YY1 is a transcription factor ubiquitously expressed in mammalian cells and has both transcriptional activation and repression ability.²⁹ miR-544 has been shown to activate the transcription of ten-eleven translocation 2 by inhibiting the expression of YY1 and therefore promoting the anti-oxidative and angiogenic abilities

of human amniotic epithelial cell-derived endothelial cell-like cells; moreover, transplantation of induced endothelial cell-like cells in which miR-544 was overexpressed has been shown to significantly reduced oxidative stress and plaque deposits in atherosclerotic mice.³⁰ These findings indicate that YY1 plays a significant role in atherosclerosis and regulates vascular endothelial cell inflammation.

In this study, the knockdown of YY1 decreased the expression of IRAK1 in LPS-treated HCAECs, indicating that YY1 is an activator of the transcription of IRAK1. IRAK1 is a well-characterized pro-inflammatory molecule. Disturbed flow has been shown to promote NCK adaptor protein 1-dependent IRAK1 activation and therefore provoke endothelial activation and atherogenic inflammation.³¹ In addition, miR-146a-5p has been shown to reduce the expressions of IRAK1 and adhesion molecules to protect human aortic endothelial cells from high glucose-induced inflammatory injury.³² Dendritic cell-derived exosomal miR-146a has been shown to reduce the adhesion and inflammation of exosome-stimulated human umbilical vein endothelial cells by inhibiting the expression of IRAK1.³³

This study provides the first evidence that miR-29b-3p suppresses LPS-induced inflammatory response of HCAECs, and demonstrates the involvement of YY1-mediated transcription of IRAK1 in this process. Previous studies have only described miR-29b-3p as a vascular regulator and also a regulator of inflammation in other disease conditions, but have not elucidated the specific role of miR-29b-3p in vascular inflammation. The YY1/IRAK1 axis is not a novel finding, but this is the first time that it has been shown to be regulated by miR-29b-3p in LPS-induced inflammatory response of HCAECs. Moreover, our *in vivo* data showed that the upregulation of miR-29b-3p suppressed the inflammatory response after intraluminal injury of the common femoral artery in rats. The experimental results of this study may, at least in part, elucidate the mechanisms of post-vascular injury inflammation and provide therapeutic targets. After validation by sufficient clinical trials, miR-29b-3p could be applied to the surface of stents to control inflammatory response, thereby reducing adverse events after PCI. Moreover, the findings about miR-29b-3p may help to develop personalized medicine for cardiovascular events.

Despite the clinical implications, this study is primarily an experimental work and needs more clinical re-

search to evaluate the findings. First, LPS-induced HCAEC inflammation may partially mimic atherogenic injury, but it is still far from mechanical vascular injury. Therefore, the experimental data should be carefully considered before further validation. A large amount of basic and clinical research should be conducted to determine whether the results of cell culture can be transferred one-to-one to humans. Second, the clinical sample size of this study is small. Studies with more clinical data are needed to further verify the correlations between the expression levels of miR-29b-3p and inflammatory factors after PCI. It would also be interesting to investigate the miR-29b-3p expression according to the type and complexity of PCI, level of coronary artery disease, presence or absence of non-reflow etc. Third, a follow-up study is required to analyze the relationships between different plasma levels of miR-29b-3p and the incidence of end-point events (e.g. cardiac death, myocardial infarction, and readmission for PCI) in ACS patients after PCI. Fourth, although the *in vitro* data clearly demonstrated that miR-29-3p repressed the YY1/IRAK1 pathway and subsequent inflammatory mediators, how vascular injury downregulates miR-29-3p expression and whether vascular inflammation itself also downregulates miR-29-3p levels is unknown.

ACKNOWLEDGEMENTS

Thanks to all the contributors.

AUTHORS' CONTRIBUTIONS

ZYY, LJY and YY conceived the ideas. ZYY, LJY and YY designed the experiments. ZYY, YY, HL and SL performed the experiments. ZYY, YY, LHL and ZFX analyzed the data. SL and LHL provided critical materials. ZYY, YY, LHL and ZFX wrote the manuscript. LJY supervised the study. ZYY and YY contributed equally to this research. All the authors have read and approved the final version for publication.

FUNDING

Not applicable.

DATA AVAILABILITY STATEMENT

The datasets used or analyzed during the current study are available from the corresponding author on reasonable request.

ETHICAL STATEMENT

Blood samples were collected and used under the approval of the ethics committee of Jiangxi Provincial People's Hospital (No. 20210209-324) and the written informed consent of all patients or their families.

CONSENT FOR PUBLICATION

The informed consent of all patients or their families were collected.

DECLARATION OF CONFLICT OF INTEREST

The authors declare there is no conflict of interest regarding this study.

REFERENCES

1. Zhao D, Liu J, Wang M, et al. Epidemiology of cardiovascular disease in China: current features and implications. *Nat Rev Cardiol* 2019;16:203-12.
2. Hedayati T, Yadav N, Khanagavi J. Non-ST-segment acute coronary syndromes. *Cardiol Clin* 2018;36:37-52.
3. Libby P, Pasternak G, Crea F, Jang IK. Reassessing the mechanisms of acute coronary syndromes. *Circ Res* 2019;124:150-60.
4. Pettersen TR, Fridlund B, Bendz B, et al. Challenges adhering to a medication regimen following first-time percutaneous coronary intervention: a patient perspective. *Int J Nurs Stud* 2018;88:16-24.
5. Shah B, Pillinger M, Zhong H, et al. Effects of acute colchicine administration prior to percutaneous coronary intervention: COLCHICINE-PCI Randomized Trial. *Circ Cardiovasc Interv* 2020; 13:e008717.
6. Lu TX, Rothenberg ME. MicroRNA. *J Allergy Clin Immunol* 2018; 141:1202-7.
7. Saliminejad K, Khorram Khorshid HR, Soleymani Fard S, Ghaffari SH. An overview of microRNAs: biology, functions, therapeutics,

- and analysis methods. *J Cell Physiol* 2019;234:5451-65.
8. Wang JN, Yan YY, Guo ZY, et al. Negative association of circulating microRNA-126 with high-sensitive C-reactive protein and vascular cell adhesion molecule-1 in patients with coronary artery disease following percutaneous coronary intervention. *Chin Med J (Engl)* 2016;129:2786-91.
 9. Pei YH, Chen J, Wu X, et al. LncRNA PEAMIR inhibits apoptosis and inflammatory response in PM2.5 exposure aggravated myocardial ischemia/reperfusion injury as a competing endogenous RNA of miR-29b-3p. *Nanotoxicology* 2020;14:638-53.
 10. Flannery S, Bowie AG. The interleukin-1 receptor-associated kinases: critical regulators of innate immune signalling. *Biochem Pharmacol* 2010;80:1981-91.
 11. Su Q, Lv X, Ye Z, et al. The mechanism of miR-142-3p in coronary microembolization-induced myocardial injury via regulating target gene IRAK-1. *Cell Death Dis* 2019;10:61.
 12. Patten M, Wang W, Aminololama-Shakeri S, et al. IL-1 beta increases abundance and activity of the negative transcriptional regulator yin yang-1 (YY1) in neonatal rat cardiac myocytes. *J Mol Cell Cardiol* 2000;32:1341-52.
 13. Li J, Yang T, Sha Z, et al. Angiotensin II-induced muscle atrophy via PPARgamma suppression is mediated by miR-29b. *Mol Ther Nucleic Acids* 2021;23:743-56.
 14. Wang H, Liu Z, Shao J, et al. Immune and inflammation in acute coronary syndrome: molecular mechanisms and therapeutic implications. *J Immunol Res* 2020;2020:4904217.
 15. Zou Y, Fu Y, Davies MG. Galphag G proteins modulate MMP-9 gelatinase during remodeling of the murine femoral artery. *J Surg Res* 2013;181:32-40.
 16. Bhatt DL. Percutaneous coronary intervention in 2018. *JAMA* 2018;319:2127-8.
 17. Giannini F, Candilio L, Mitomo S, et al. A practical approach to the management of complications during percutaneous coronary intervention. *JACC Cardiovasc Interv* 2018;11:1797-810.
 18. Kereiakes DJ. Adjunctive pharmacotherapy before percutaneous coronary intervention in non-ST-elevation acute coronary syndromes: the role of modulating inflammation. *Circulation* 2003;108:III22-7.
 19. Dunzendorfer S, Lee HK, Soldau K, Tobias PS. Toll-like receptor 4 functions intracellularly in human coronary artery endothelial cells: roles of LBP and sCD14 in mediating LPS responses. *FASEB J* 2004;18:1117-9.
 20. Zeuke S, Ulmer AJ, Kusumoto S, et al. TLR4-mediated inflammatory activation of human coronary artery endothelial cells by LPS. *Cardiovasc Res* 2002;56:126-34.
 21. Jiang W, Zhang Z, Yang H, et al. The involvement of miR-29b-3p in arterial calcification by targeting matrix metalloproteinase-2. *Biomed Res Int* 2017;2017:6713606.
 22. Jiang W, Zhang Z, Yang H, et al. The miR-29b/matrix metalloproteinase 2 axis regulates transdifferentiation and calcification of vascular smooth muscle cells in a calcified environment. *Blood Purif* 2020;49:524-34.
 23. Ma Q, Zhang J, Zhang M, et al. MicroRNA-29b targeting of cell division cycle 7-related protein kinase (CDC7) regulated vascular smooth muscle cell (VSMC) proliferation and migration. *Ann Transl Med* 2020;8:1496.
 24. Marques FZ, Vizi D, Khammy O, et al. The transcardiac gradient of cardio-microRNAs in the failing heart. *Eur J Heart Fail* 2016;18:1000-8.
 25. Leistner DM, Boeckel JN, Reis SM, et al. Transcoronary gradients of vascular miRNAs and coronary atherosclerotic plaque characteristics. *Eur Heart J* 2016;37:1738-49.
 26. Zhi L, Zhao J, Zhao H, et al. Downregulation of LncRNA OIP5-AS1 induced by IL-1beta aggravates osteoarthritis via regulating miR-29b-3p/PGRN. *Cartilage* 2020;1947603519900801.
 27. Dai Y, Mao Z, Han X, et al. MicroRNA-29b-3p reduces intestinal ischaemia/reperfusion injury via targeting of TNF receptor-associated factor 3. *Br J Pharmacol* 2019;176:3264-78.
 28. Wang J, Zhu M, Ye L, et al. MiR-29b-3p promotes particulate matter-induced inflammatory responses by regulating the C1QTNF6/AMPK pathway. *Aging (Albany NY)* 2020;12:1141-58.
 29. Verheul TCJ, van Hijfte L, Perenthaler E, Barakat TS. The why of YY1: mechanisms of transcriptional regulation by Yin Yang 1. *Front Cell Dev Biol* 2020;8:592164.
 30. Guo J, Xiang Q, Xin Y, et al. miR-544 promotes maturity and antioxidation of stem cell-derived endothelial like cells by regulating the YY1/TET2 signalling axis. *Cell Commun Signal* 2020;18:35.
 31. Alfaiidi M, Acosta CH, Wang D, et al. Selective role of Nck1 in atherogenic inflammation and plaque formation. *J Clin Invest* 2020;130:4331-47.
 32. Lo WY, Peng CT, Wang HJ. MicroRNA-146a-5p mediates high glucose-induced endothelial inflammation via targeting interleukin-1 receptor-associated kinase 1 expression. *Front Physiol* 2017;8:551.
 33. Zhong X, Gao W, Wu R, et al. Dendritic cell exosomes shuttle miRNA146a regulates exosome-induced endothelial cell inflammation by inhibiting IRAK1: a feedback control mechanism. *Mol Med Rep* 2019;20:5315-23.